Combustion and Flame 199 (2019) 249–257

Contents lists available at ScienceDirect

Combustion and Flame

journal homepage: www.elsevier.com/locate/combustflame

Temperature measurements under diesel engine conditions using laser induced grating spectroscopy

F. Förster[a], C. Crua[b], M. Davy[c], P. Ewart[a,*]

[a] Department of Physics, Clarendon Laboratory, University of Oxford, OX1 3PU, UK
[b] Advanced Engineering Centre, University of Brighton, BN2 4GJ, UK
[c] Department of Engineering Science, University of Oxford, OX1 3PJ, UK

ARTICLE INFO

Article history:
Received 28 March 2018
Revised 11 October 2018
Accepted 12 October 2018

Keywords:
Combustion diagnostics
Diesel combustion
Thermometry
Laser induced grating spectroscopy

ABSTRACT

Crank angle-resolved temperatures have been measured using laser induced grating spectroscopy (LIGS) in a motored reciprocating compression machine to simulate diesel engine operating conditions. A portable LIGS system based on a pulsed Nd:YAG laser, fundamental emission at 1064 nm and the fourth harmonic at 266 nm, was used with a c.w. diode-pumped solid state laser as probe at 660 nm. Laser induced thermal grating scattering (LITGS) using resonant absorption by 1-methylnaphthalene, as a substitute fuel, of the 266 nm pump-radiation was used for temperature measurements during non-combusting cycles. Laser induced electrostrictive grating scattering (LIEGS) using 1064 nm pump-radiation was used to measure temperatures in both combusting and non-combusting cycles with good agreement with the results of LITGS measurements which had a single-shot precision of ± 15 K and standard error of ± 1.5 K. The accuracy was estimated to be ± 3 K based on the uncertainty involved in the modified equation of state used in the derivation from the LIGS measurements of sound speed in the gas. Differences in the in-cylinder bulk gas temperature between combusting and non-combusting cycles were unambiguously resolved and temperatures of 2300 ± 100 K, typical of flames, were recorded in individual cycles. The results confirm the potential for LIGS-based thermometry for high-precision thermometry of combustion under compression-ignition conditions.

1. Introduction

The temperature of gases in combustion engines is a critical parameter in determining the performance in many respects. The efficiency of any heat engine is determined, *inter alia*, by the range of temperatures of the 'working fluid' during the cycle and the temperature before ignition affects the evaporation of injected fuel and its mixing with air such as to influence the completeness of combustion and generation of particulate matter in the exhaust. Furthermore, the rate of many chemical reactions is temperature dependent and the level of pollutants created in air-fed combustion, such as NOx, is highly dependent on temperature. The accurate and precise measurement of gas temperature is therefore an important diagnostic tool for development of more efficient and less polluting engines and fuels.

Legislation mandating lower emissions of CO, CO_2, NO_X, and particulate matter (PM) has been driving research in emissions control by both in-cylinder methods including fuel/air management and exhaust gas recirculation (EGR) and exhaust aftertreatments. Conventional methods have typically involved a trade-off between emissions of NO_X and PM but more radical approaches are currently under development utilizing alternative combustion strategies such as split-cycle engines and novel compression ignition technology. These novel approaches can involve operation with very high levels of EGR, supercritical conditions at the start of fuel injection, much higher turbulence levels and at greatly increased peak pressure and temperature.

Thermometry in such technical combustion devices presents significant experimental challenges including high pressure environments, temperature ranges from 300 to 2000 K and limited optical access. A number of non-invasive, optical methods have been employed in recent decades to address these difficulties including Coherent Anti-Stokes Raman Spectroscopy (CARS), Laser Induced Fluorescence (LIF) and Tunable Diode Laser Absorption Spectroscopy (TDLAS) [1]. More recently, Laser Induced Grating Spectroscopy (LIGS) or Laser Induced Thermal Acoustics (LITA) has emerged as a technique offering improved precision compared to other optical methods [2–8]. LIGS has been shown to provide measurement uncertainty of the order of 1%, sufficient to distinguish differences in evaporative cooling of gasoline-alcohol blends

* Corresponding author.
E-mail address: p.ewart@physics.ox.ac.uk (P. Ewart).

https://doi.org/10.1016/j.combustflame.2018.10.017
0010-2180/

differing by only 5% in alcohol content, in a firing gasoline-fuelled, direct-injection spark ignition (DISI) engine [9]. The technique has also been successfully applied to calibration of Two-Colour Planar Laser Induced Fluorescence imaging of temperature distributions in a firing engine [10]. Recent developments have also included applications in shock tubes and high-speed fuel injection jets and mixing [11,12].

Engines operating under diesel-like conditions present particularly severe challenges for optical techniques. The very high pressures encountered in compression ignition engines seriously compromise fluorescence-based methods owing to the rapid, and poorly quantified, quenching effects that reduce signal levels and make quantitative measurements of intensity difficult to interpret in terms of temperature or concentration. Accurate knowledge of spectral line broadening effects is also critical for quantitative interpretation of CARS and TDLAS signals and such information is not usually available for the range of temperatures, compositions and pressures encountered in diesel combustion situations. A general disadvantage of many of these methods arises from their dependence upon measurement of relative intensities, or spectral distribution of intensity, since such measurements are adversely affected by random fluctuations in the incident laser intensity and scattering from particles or surfaces or other sources of noise. The techniques of LIGS and LITA, however, are based on measurement of frequency of the oscillations in the detected signal and are therefore less susceptible to effects of intensity noise. Since frequencies are more easily measured accurately than intensities, these techniques offer improved precision in the temperature derived from the signal. Furthermore, the strength of the signal in LIGS processes increases with increasing pressure, in contrast to most other optical methods where increasing pressure usually leads to weaker signals. This characteristic of LIGS will be of particular advantage in diesel-like conditions where high pressures are commonly encountered. On the other hand, it should be admitted that high pressure conditions can lead to difficulties since accurate knowledge of gas dynamic parameters is required in order to derive the temperature accurately from the measured frequency and such information is often not available, especially at elevated temperatures and pressures. In addition, some of the assumptions used in the usual derivation of temperature from LIGS signals may not be valid under such conditions and a modification to the usual equation-of-state (EoS) may be required.

In order to develop accurate phenomenological and mathematical models for the formation and combustion of fuel sprays, it is essential that researchers can perform controlled experiments with well-defined boundary conditions. Such measurements are normally performed in constant-volume or constant-flow spray vessels, rapid compression machines (RCMs), or optical engines. The time-resolved gas pressure inside these research facilities can easily recorded using high-accuracy piezo-resistive pressure sensors. However, obtaining information about the gas temperature is much more challenging due to the short timescales involved. In constant-volume spray vessels the relatively slow temperature decay timescales make it possible to characterise the temperature field of the gas phase using thin-wire thermocouples [13]. Even though the hot junctions are in the order of 25–50 µm, it is necessary to use appropriate corrections for the thermal inertia of the thermocouple and the radiative heat transfer between the thermocouple and the vessel, as these are not negligible for typical diesel operating conditions. In the case of optical engines and RCMs the timescales are significantly faster and require thermocouples with hot junctions smaller than 25 µm. Nilaphai et al. recently used 13 µm thermocouples in an RCM although this particular research facility operates on a single-shot basis [14]. Successfully mounting and using such thin thermocouples for any extended periods of time remains a significant challenge, even though the stress on the thin wires is not as limiting as it would be in a reciprocating RCM or optical engine where running times are several orders of magnitude longer.

Laser diagnostics can provide non-intrusive, and potentially multi-dimensional, measurements of gas as well as flame temperature in such challenging operating conditions. Laser Rayleigh scattering can provide single-shot accuracies of the order of 30 K but any background Mie scattering must be prevented or removed, thus making it particularly challenging for reciprocating machines and optical engines, and unsuitable for flame temperature measurement [15]. Since the fluorescence signals of compounds such as acetone and toluene are highly sensitive to temperature, Planar Laser-Induced Fluorescence (PLIF) can be implemented to characterise a temperature field when the intake air is seeded with such tracers [16]. Such single-wavelength detection strategies can provide uncertainties as low as ± 4 K but require the pegging to a known temperature either through a secondary measurement or through thermodynamic calculation [15]. Since corrections for tracer concentration, laser fluence and absorption are also required [17], a dual-wavelength measurement is often preferred even though this approach is more complex and offers lower sensitivities and precisions [18,19]. Toluene has become a tracer of choice for PLIF thermometry due to its high fluorescence quantum yield, even though the yield exponentially decreases with increasing temperatures [20,17].

There are three major limitations for toluene PLIF as a temperature diagnostic for reciprocating RCMs and optical engines. First, the strong collisional quenching of toluene LIF by molecular oxygen must be suppressed. For reciprocating RCMs and engines the mass flow rates of nitrogen required to achieve this can be particularly significant, thus limiting running durations. Second, and more importantly for combustion studies, the need for an inert environment inevitably precludes the possibility of temperature measurements under reactive conditions. Third, the crank-resolved measurement of temperatures by toluene LIF requires a short pulse laser beam at 266 nm which typically have low energies. This leads to the requirement for relatively high concentrations of toluene, whose condensation becomes significant and intrusive as it causes heterogeneities in local mixture fraction inside the combustion chamber [18].

Hence there is a need to develop non-intrusive temperature diagnostic techniques for the particularly challenging operating conditions found in reciprocating fuel combustion research facilities. LIGS appears to be a promising technique which doesn't require inert environments, can be applied at acquisition rates of 10 kHz, and can be applied using alkane tracers that are more representative of diesel fuels [21,22]. The technique may be applied using fuel/air mixtures with or without an added "tracer" species to act as absorber or, as explained below, in pure air.

In this paper we report the first application of LIGS to thermometry under diesel engine conditions. We demonstrate the use of a portable system for making LIGS measurements in a technical combustion device using signals based on Laser Induced Thermal Grating Scattering (LITGS) and Laser Induced Electrostrictive Grating Scattering (LIEGS). The LITGS process uses a resonant absorption process to produce the grating in which the excitation energy absorbed by a suitable molecular species is translated into the grating by collisional quenching. In the LIEGS process the mechanism for grating production is from the electrostrictive effect – a non-resonant process that leads to the transient perturbation of the medium refractive index. The non-resonant character of LIEGS enables signals to be generated in the absence of an absorbing species and allows measurements in both unburnt and burnt gas during compression cycles in which combustion occurs.

2. Experimental methods

2.1. Test facility

The experiments were carried out using a reciprocating rapid compression machine based around a Ricardo Proteus single cylinder engine converted to liner-ported, 2-stroke cycle operation [23]. The machine offers a relatively large optical access compared to conventional light-duty optical engines, and significantly higher fuel injection frequency compared to a constant-volume spray vessel.

The removal of the valve train allowed the fitting of an optical chamber of 80 mm in height and 50 mm diameter into the cylinder head. The optical access to the combustion chamber was provided by up to three removable sapphire glass windows. As a result of the increased volume of the combustion chamber the compression ratio was reduced to 9:1. To simulate a diesel-like operating conditions the intake air was conditioned to give in-cylinder pressures and temperatures up to 8 MPa and 900 K, respectively. Prior to motoring, the cylinder head was heated by a water jacket to 85 °C and immersion heaters heated the oil to 40 °C. The machine was motored by a dynamometer to 500 rpm, and kept at stable in-cylinder conditions for the duration of the recordings. Scavenging on the in-cylinder gases was done by skipping injections for several cycles. This approach still allowed an acquisition frequency of several fuel injections per second. The in-cylinder pressure was recorded as a function time of using a high-accuracy piezo-resistive pressure sensor.

The fuel was delivered by a Delphi common-rail system, comprising a DFP-3 high-pressure pump rated at 200 MPa, and a single axial hole Bosch injector with a sac-type nozzle (ECN Spray A type nozzle). The high-pressure rail and the delivery pipe were both instrumented with pressure transducers. The rail pressure, timing and duration of the injections were independently controlled by a National Instruments fuel injection controller.

2.2. Optical arrangements and procedures for LIGS

The principles and practical arrangements for generating LIGS signals have been reviewed recently and so here we outline only briefly the salient features [24]. A grating-like pattern is created by the interference of two, pulsed, laser beams crossing at a small angle. The refractive index of the medium is modified by the interaction with the light in the high-field regions of the pattern. The transient perturbation of the medium's density and temperature creates a stationary grating with a spatial periodicity defined by the wavelength and crossing angle of the beams. Simultaneously a standing acoustic wave is launched – a result of two oppositely propagating sound waves. In the case where the pump radiation is resonantly absorbed (LITGS) a stationary thermal grating is established as collisional quenching transfers energy from molecular excited states to the bulk medium. This grating decays exponentially at a rate determined by molecular diffusion. The scattering efficiency of the induced grating is modulated as the standing acoustic wave evolves periodically in and out of phase with the stationary grating. This modulation has a frequency determined by the transit time of the sound waves across the stationary grating and decays exponentially owing to viscous damping effects. The grating evolution and decay is detected by recording the intensity of light scattered from a probe beam incident at the appropriate Bragg scattering angle. This scattered light constitutes the signal in the form of a decaying sinusoidal oscillatory intensity on an exponentially decaying background. In the case of non-resonant (electrostrictive) interaction the stationary thermal grating is absent and so the acoustic oscillations are observed on a zero-background and thus appear at twice the frequency of the thermal grating signals [2–4].

As noted above, the spatial periodicity of the grating, Λ, is set by the crossing angle, θ, and wavelength, λ, of the pump beams:

$$\Lambda = \frac{\lambda}{2\sin(\theta/2)} \tag{1}$$

The modulation frequency, f_{osc}, determined by the local sound speed c_S, is given by,

$$f_{osc} = c_S/\Lambda \tag{2}$$

The temperature, T, may be derived from the speed of sound provided that the relationship, characterised by an appropriate equation of state (EoS), between T and c_S is known. Under diesel-like conditions of high pressure the usual EoS based on the Ideal Gas laws is not appropriate and leads to significant errors in the temperature derived from the measured sound speed. Over the range of pressure from 1 to 100 bar the speed of sound varies by up to 6% and so a more realistic EoS must be employed. In this work the relevant information for binary mixtures in dry air were obtained using the NIST REFPROP data base [25]. In the experiments reported here the assumption of dry air was verified using a humidity sensor in the air intake.

The procedure for obtaining a temperature measurement using LIGS is therefore to excite the grating resonantly or non-resonantly and record the time behaviour of the Bragg-scattered light from a probe beam. The oscillation frequency, f_{osc}, is then obtained by a suitable process such as a fast Fourier transform of the recorded signal and, from a knowledge of the grating spacing, Λ, the local sound speed, c_S, is derived. The temperature is then derived using an appropriate equation of state as outlined above.

2.2.1. Optical set-up

A compact and portable laser and optical system comprised of a small Nd:YAG laser (Continuum Minilite II) as pump laser and a diode pumped solid state laser (Laser Quantum Ventus 660) was mounted adjacent to the RCM on a 3-axis electronic stage with 3 µm positioning accuracy.

The system for generating LITGS signals used the fourth harmonic of the Nd:YAG laser providing pulses of 8 ns duration and 4 mJ total energy at 266 nm. The output of the DPSS laser provided up to 750 mW power at 660 nm for the probe laser. The optical system generated two pump beams, the probe beam and a 'dummy' signal beam for alignment purposes, which were crossed at the measurement point by a 300 mm focal length "crossing" lens. The separation of the pump beams and probe beams at the crossing lens were adjusted with the aid of alignment masks to produce a grating spacing, Λ, appropriate to give signal oscillation frequencies in the range of 10–100 MHz. The beams were transmitted by fused silica windows in the RCM and the measurement point, selected by adjustment of the 3-axis electronic translation stage, was chosen to lie on the axis of the fuel injector as shown in Fig. 1. The signal emanating from the interaction region was transmitted by an opposing window and directed to a photomultiplier tube (Hammamatsu H10721), the output of which was recorded on a digital oscilloscope (LeCroy Waverunner 625Zi) having a bandwidth of 250 MHz. No significant deviation of the signal beam arising from "beam steering effects" was observed during operation of the RCM.

For recording of LIEGS signals the fundamental output of the Nd:YAG laser was used consisting of pulses of approximately 80 mJ energy at 1064 nm and with duration of 5–7 ns. The quartz optics were replaced, where appropriate, with BK7 glass components and suitably reflecting mirrors and beam splitters. The same DPSS laser at 660 nm was used as the probe with a crossing lens of 750 mm focal length. A suitable alignment mask system was used for alignment purposes at this different wavelength in order to generate a grating with a suitable periodicity.

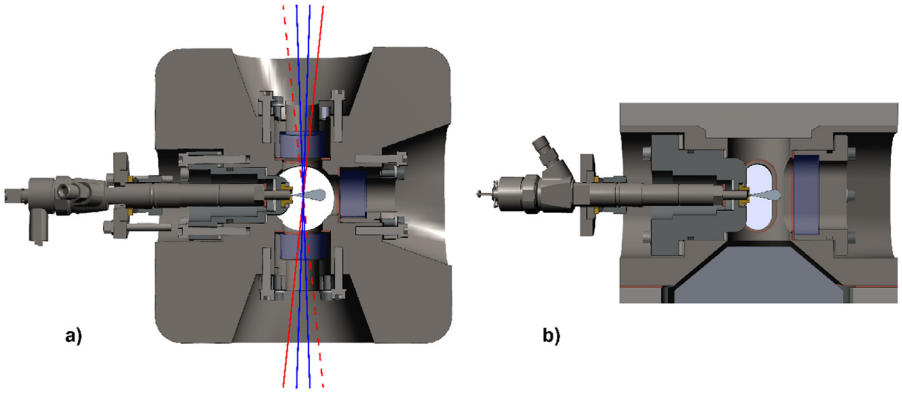

Fig. 1. Location of measurement volume, defined by the intersection of the pump beams (blue lines) and probe beam (red solid line). (a) plan view and (b) elevation view, showing position of the measurement volume relative to the injector nozzle in the left-hand wall of the chamber. The dashed red line shows the direction of the beam used to trace the signal beam and which is blocked during the taking of data. (For interpretation of the references to colour in this figure legend, the reader is referred to the web version of this article.)

2.2.2. Measurement resolution, accuracy and precision

The geometry of the pump and probe beams determines the spatial resolution of the measurement. The diameter and crossing angles of the pump beams are the primary factors defining the interaction and measurement volume. The crossing angle for the resonant LIGS (266 nm pumps) was 2.67° and for LIEGS (1064 nm pumps) the angle was 2.75° with beam diameters of approximately 200 μm. The maximum longitudinal extent of the interaction region is thus estimated to be 8 mm. However, owing to the rhomboidal shape of this region, the majority of the signal is generated in the central section and the effective spatial resolution is estimated to be a region of 200 μm diameter and 4–5 mm in axial extent, i.e a volume of approximately 0.5 mm^3. This represents reasonable spatial resolution relative to the total chamber volume of 6.3×10^5 mm^3.

The temporal resolution is determined by the duration of the LIGS signals generated over the range of pressures encountered in the compression which varies from about 200 ns to less than 1 μs. This time scale is effectively instantaneous relative to the other time scales involved in the turbulent flow within the optically accessible chamber.

The accuracy of temperature values derived from LIGS signals depends upon accurate knowledge of the grating spacing, Λ. In practice, although this may be calculated from geometrical measurements of the beam arrangements, a more accurate value is found by measurement of temperature in a controlled environment where the temperature and gas composition is accurately known. In the present work this was accomplished using a purpose-built optical test cell at temperatures measured by an accurate thermocouple. The accuracy of this calibration procedure is determined by the precision of the measurement of the local sound speed derived from the LIGS signal frequency according to Eq. (2). The absolute accuracy in derived temperature values is ultimately limited by uncertainty in the accuracy of the Equation of State used to relate the measured local sound speed to the local temperature value.

The inherent precision of the measurements was determined by recording LIGS signals in a stable environment i.e. a test cell at constant temperature and pressure. The measurement of the oscillation frequency that is obtained from the LITGS or LIEGS signals is a direct measurement of the local speed of sound. Under conditions of constant temperature, pressure and composition in the test cell the speed of sound will be a constant, determined by the thermodynamic parameters of the gas, and this provides the calibration value. The variation in the single-shot measurement values relative to the constant calibration value is shown by the histogram in Fig. 2. This data shows that the inherent precision in single-shot values of the sound speed, measured under these stable conditions, has a value of 0.25% and this translates into a corresponding precision in the single-shot values of temperature derived from both LITGS and LIEGS signals.

2.2.3. Resonant LIGS

The principal advantage of using resonant LIGS, in which a thermal grating is established by absorption and collisional quenching, is that strong signals are more easily produced with quite modest input powers in the pump beams. The main disadvantage is that the molecular species used to absorb the input energy is consumed in the combustion process and so no signals can be produced in the flame regions or post-combustion phases. Using absorbers such as acetone or toluene at concentration levels around a few percent in the injected fuel/air mixture, strong LIGS signals may be produced using typically only 2–4 mJ of energy at the wavelength of the fourth harmonic of a Nd:YAG laser. Other absorbers, such as liquid alkanes e.g. hexane, may be chosen to match each of the harmonics of the Nd:YAG lasers typically used. The use of the fourth and third harmonics, 266 nm and 355 nm respectively, mandates the use of UV transmitting optics.

Initial experiments using toluene/dodecane blends proved unsuccessful owing to the tendency of the mixtures to ignite under compression and, more seriously, for the fuel mixture to provide insufficient lubrication of the fuel pumps servicing the RCM. Since the UV-absorbing component is associated with molecules containing a benzene ring a naphthalene substitute was used – specifically, 1-methylnaphthalene ($C_{10}H_8$). As a simple polycyclic aromatic hydrocarbon, 1-methylnaphthalene is a not untypical component of diesel fuels and has been identified in the literature as a suitable LIF tracer for diesel engine applications [26]. The presence of this species provides therefore a better match for standard diesel fuels and offers the same advantage as toluene does for gasoline engine measurements by acting as a tracer for both LIGS and LIF simultaneously [27,10].

The LIGS signals generated using the resonant absorption process, as described above, consist of a decaying sinusoidal oscillation superimposed on an exponentially decaying intensity arising from the interference of the acoustic and stationary thermal gratings. This signal mode, having two components at the same frequency, is sometimes referred to as homodyne detection.

2.2.3. Non-resonant LIGS

The principal advantage of using electrostrictive gratings rather than thermal gratings is that no resonant absorber is required. Therefore, in principle, signals may be generated in both pre- and

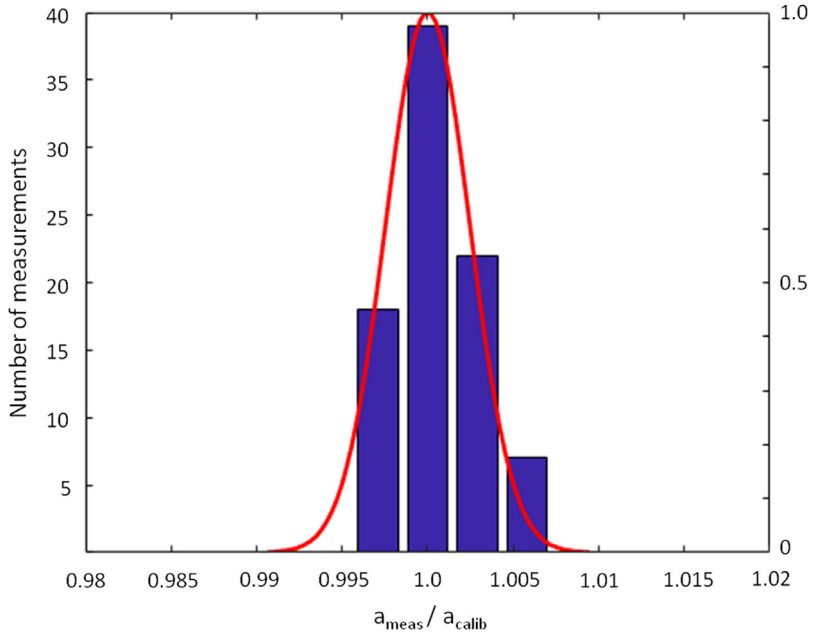

Fig. 2. Calibration data obtained in static cell under stable temperature and pressure conditions and used to specify the single-shot precision of the LIGS measurements. The histogram shows the number of measurements yielding the ratio of the measured local sound speed to the calibration value at STP, a_{meas}/a_{calib}.

post-combustion gases and even in the flame regions themselves. The main disadvantage is that the signals are usually much weaker than with resonant LIGS and the lower signal-to-noise ratio may reduce the precision of the frequency determination, especially at higher temperatures where signals are weaker owing to lower density and decay more rapidly as a result of faster diffusion.

In the experiments reported here the fundamental output of the Nd:YAG laser was used and the fuel injected into the RCM contained no added absorber species. It was assumed that absorption by the fuel at 1064 nm would not be sufficient to generate a significant thermal grating signal. The signals, therefore, arising from LIEGS, consisted of light scattered only from the induced acoustic waves in the medium. The detection scheme in this case is sometimes referred to as non-homodyne.

3. Results

3.1. UV – LITGS for cycle-resolved temperatures: non-reactive conditions

Charges of pure 1-methylnaphthalene, to act as the absorber, were injected at a crank angle degree (CAD) of 90° before top-dead-centre (TDC). The quantity of 1-methylnaphthalene injected was adjusted by variation of the injection duration and ranged over pulses from 100 to 4000 µs. For indication, a 1000 µs injection corresponded to 1 mg of liquid naphthalene in about 4 g of air. The absorber/fuel was injected during the cycle before the LIGS measurement was made. The turbulence arising from the injection and intake and exhaust strokes results in a highly uniform mixture at the time of measurement.

The single-shot precision of the measurements was determined, as described above in Section 2.2.2 to be ± 15 K with a standard error on the mean of less than ± 2.5 K. The inherent accuracy of the derived temperatures is estimated to be ± 3 K based on the uncertainty involved in the Equation of State (EoS) data in the relevant temperature and pressure range [28]. Inaccuracy can, however, be introduced if the absorption of energy in the LIGS signal generation leads to local heating in the measurement volume. Such local heating effects will be affected by the degree of absorption of energy from the pump pulses and thus on the concentration of the absorbing species – the 1-methylnaphthalene. Increasing the absorber concentration will lead to increase in the absorbed energy and so, potentially, to an increase in local temperature.

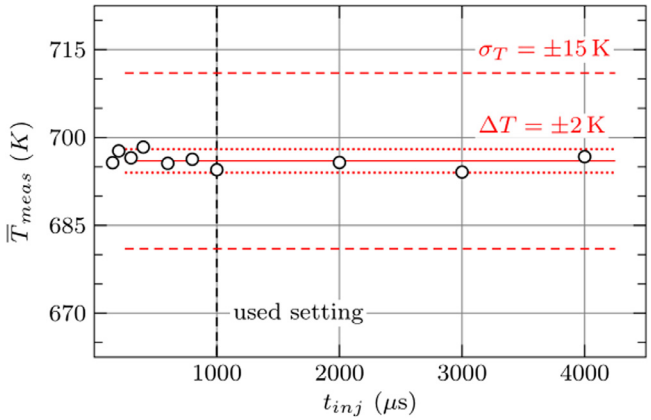

Fig. 3. Temperatures derived from LIGS data averaged over 30–80 shots for different injection durations to vary the concentration of absorber. The data shows no systematic shift of the derived temperature as a function of absorber concentration, indicating that changes in amount of absorbed energy does not significantly perturb the local temperature in the measurement volume.

In order to verify that there were no perturbations to the derived temperature arising from this local heating, the temperature was derived for each concentration of injected absorber. Measurements were made at TDC where the pressure was 60 bar. Figure 3 shows the mean temperature values, averaged over 30–80 shots, derived from the LITGS signals for the range of 1-methylnaphthalene charges injected. The data shows consistent mean values of temperature around 695 K with a variation of only 2 K over the range that is well within the standard deviation of each of the individual measurements of ± 15 K. These data show

that there was no significant perturbation of the temperature arising from absorption of the laser energy and the measurement technique is verified to be non-invasive. Furthermore, the standard deviation on the mean of ± 15 K, given the inherent precision of the measurement of ± 2.5 K, gives a measure of the reproducibility (or variability) of the conditions produced by the RCM.

Variation in gas composition in the measurement volume may also contribute to errors in the derived temperature as a result of the associated variation in the relationship between the speed of sound and temperature via the equation of state. Changes in composition arising from variation in the fuel/air ratio arise from associated changes in the ratio of specific heats, γ, and mean molecular mass m. In previous work, using LIGS to study evaporative cooling effects in gasoline direct injection engines, it was shown that errors due to uncertainty in gas composition can be minimized if the fuel concentration is kept below a certain level [9]. In the present work the amount of fuel injected was a small proportion of the overall mass of gas (air) and the data shown in Fig. 3 indicates that changes in the fuel/air ratio did not affect the derived temperature when the ratio γ/m was assumed to be constant. This insensitivity to gas composition was maintained in all the non-combusting situations studied here even at the highest concentrations of fuel injected. The situation when combustion occurs is, in general, more complicated since the exact composition may not be known if the measurement volume contains a flame or post-combustion gases. However, in the cases where combustion occurs, as will be discussed below, the amount of fuel constituted a small fraction of the total gas mixture. It is worth noting that if the LIGS technique is to be applied more generally, and specifically in situations where the fuel concentration does have a significant effect upon the relationship between sound speed and local temperature, then care must be exercised. In such cases appropriate calibration measurements are required to take account of changes in the gas dynamic properties of the gas mixture and the associated systematic error that would be introduced to the derived temperature if the effect was ignored.

Crank-angle-resolved measurements of temperature were made on the centre-line of the optical chamber over a series of RCM cycles in which the TDC pressure was maintained at 60 bar and with inlet air temperatures of 313 K (40°C) and 373 K (100 °C). Reliable signals with adequate signal-to-noise ratio were obtained only between −80–+ 80 CAD where the temperature was high enough to vaporize sufficient quantities of the naphthalene. The results are shown in Fig. 4 where it can be seen that the temperature evolution through the cycle shows the same trend for both inlet air temperatures. Each data point represents the average of a series of typically over 30 single shots. The lower panel in Fig. 4 shows the standard deviation of the single shots in each set used to derive the average value.

Thermodynamic simulations of the compression indicate that the bulk gas temperature is expected to be 685 K. The LIGS measurements, made on the centre-line of the chamber, reflect the core gas temperature which is expected to be higher than the computed bulk temperature. This is consistent with the measured temperature, derived from the LIGS signals, of 695 K (for the case of inlet air temperature of 40 °C as shown in Fig. 4.

As noted above, the temperature measurements are derived from single-shot data giving a measure of the instantaneous temperature. The precision of these measurements varies between ± 5 K and ± 15 K as indicated by the standard deviation. Since the measurements are made only once in a given compression cycle of the RCM it is not possible to use the measurements to provide data for turbulence statistics. It is, however, possible to obtain time-resolved measurements within a given compression stroke using a higher repetition rate laser system. Previous work has shown that accurate and precise, time-resolved, temperatures

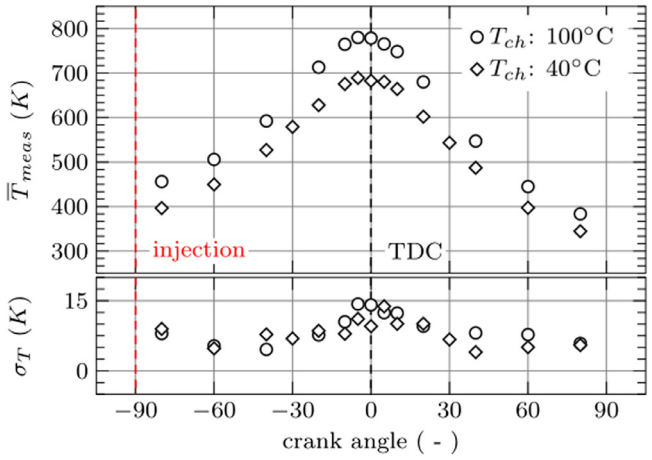

Fig. 4. Mean temperatures derived from LITGS signals in 1-methylnaphthalene/air mixture in the chamber for inlet air temperatures of 40°C and 100°C. The vertical dashed line indicates the time of injection of the 1-methylnaphthalene at −90 CAD. The lower panel shows the variation of the standard deviation of single-shot temperatures over the cycle. Data is available during the range −80–+ 80 CAD owing to the need for sufficient temperature rise by adiabatic compression to provide sufficient vapour density (see text for details.).

data can be obtained at acquisition rates of up to 10 kHz [21]. Such high repetition-rate measurements could be used to study turbulence.

3.2. IR – LIEGS for cycle-resolved temperatures: non-reactive conditions

The laser system was modified, by removing the frequency quadrupling components, and the IR-output at 1064 nm was used to provide the pump beams as outlined above. The same set of measurements was then made as for the UV-LITGS experiments with the added advantage that, since there was no minimum temperature required to produce adequate vapour density, there was no limitation on the range of CAD that could be investigated. Data was again acquired for different air intake temperatures and with compression producing 60 bar at TDC on all non-combusting cycles.

For comparison, the temperature values derived using the UV-LITGS measurements and the data derived from the IR-LIEGS measurements is shown in Fig. 5. As explained above, the LITGS data is available only over the range −80–+ 80 CAD. The inlet conditions corresponding to this data included a nominal air inlet temperature of 40 °C and pressure of 60 bar at TDC. The slight asymmetry in the temperature profiles reveals the effect of loss due to piston 'blow-by' during the compression stroke and vividly illustrates the precision of the technique. Such features will be important for validation of numerical simulations and CFD-modelling of the compression and expansion cycles.

3.3. IR – LIEGS for cycle-resolved temperatures: with combustion

In order to generate combustion conditions, injections of dodecane were introduced to provide combustible mixtures using the same compression conditions as above i.e. 60 bar at TDC and a nominal inlet air temperature of 132 °C. A sequence of four injections, each of duration 2000 µs, were made at 23, 17, 11, 5 CAD before top dead centre, BTDC. Reproducible conditions for each combustion cycle were arranged by adopting the following skip-injection sequence; a measurement was made (i) on a non-combustion cycle i.e. no fuel injected, (ii) with fuel injection to

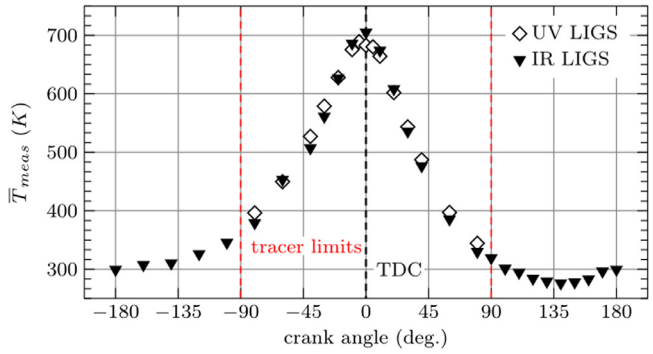

Fig. 5. Mean temperatures in the chamber for inlet air temperatures of 40 °C derived from LITGS signals in 1-methylnaphthalene/air mixture using UV-excitation (open diamond symbols). The vertical dashed red lines indicate the range over which the vapour density of the 1-methylnaphthalene provided adequate signals (see text for details).) The mean temperatures in the chamber for the same inlet air temperatures of 40°C derived from LIEGS signals using IR-excitation are shown as solid triangle symbols. (For interpretation of the references to colour in this figure legend, the reader is referred to the web version of this article.)

initiate combustion (iii) a purge cycle to remove residual combustion products and (iv) a second purge cycle to purge residuals. The scavenging efficiency was measured to be 67% and since injections were performed once in every three cycles the level of residuals present in the chamber during measurement cycles was less than 4%. Residuals at this level were found to have negligible effect on the derived temperatures in line with previous measurements in GDI engines [9].

Measurements were made over such sequences of combusting and non-combusting cycles to demonstrate that data could be acquired in the presence of combustion – a feature that would not be possible using LITGS where the absorber species would be consumed by the combustion.

The results are shown in Fig. 6. Figure 6(b) in particular shows the influence on the bulk-gas in-cylinder temperature when combustion occurs. The data shown are averages over 30 single-shot measurements with the exception of the points at −10 and −5 CAD BTDC where slightly fewer measurements were used. The error bars in Fig. 6(b) represent twice the standard deviation i.e. 95% confidence interval. The data points for cycles containing a combustion event show an elevated temperature after TDC compared to non-combusting cycles. It should be noted that the higher temperature in the combusting cycles does not indicate the flame temperature but rather the temperature rise of the bulk gas due to the combustion of a small quantity of fuel within it. The small value of the temperature increase of the bulk gas is reflected also in the small change in pressure when combustion occurs as shown in the pressure trace of Fig. 6(c). Nonetheless, again, we note the technique is capable of detecting and measuring the relatively small temperature difference with high precision.

The LIEGS signals are typically weaker than those generated by the LITGS process and so the signal-to-noise ratio is reduced. Nonetheless, Fourier analysis of the signals reveals a single dominant frequency corresponding to a single temperature in the measurement volume. Examination of individual LIEGS signals showed that occasionally the signal was dramatically different from the majority of the signals. An example is shown in Fig. 7(b) in comparison to a more typical LIEGS signal in Fig. 7(a). The most obvious features are firstly that the signal is dramatically shorter in duration and secondly the oscillation frequency is markedly higher. These are features of LIGS signals at elevated temperature. The higher frequency reflects the higher speed of sound associated with higher temperature and the more rapid decay of the signal is the symptom of faster diffusion that is characteristic of higher temperatures. As indicated in the figure, the temperature derived from these signals of 2300 ± 100 K is typical of flame temperatures or those of post-flame gases. Given that the environment in the RCM gives rise to vortices and turbulence that displace the flame fronts from the combustion sites unpredictably, the measurement volume will contain a flame or hot combustion products only on random occasions. These data, however, do show that the LIEGS technique is capable of recording flame or post-flame temperatures as well as those of the bulk gas in both combusting and non-combusting cycles.

It is worth noting here that the derivation of the temperature from the LIEGS signal in the cases where combustion has occurred has assumed a gas composition and γ/m value typical of diesel flames. The uncertainty in these values is reflected in the larger

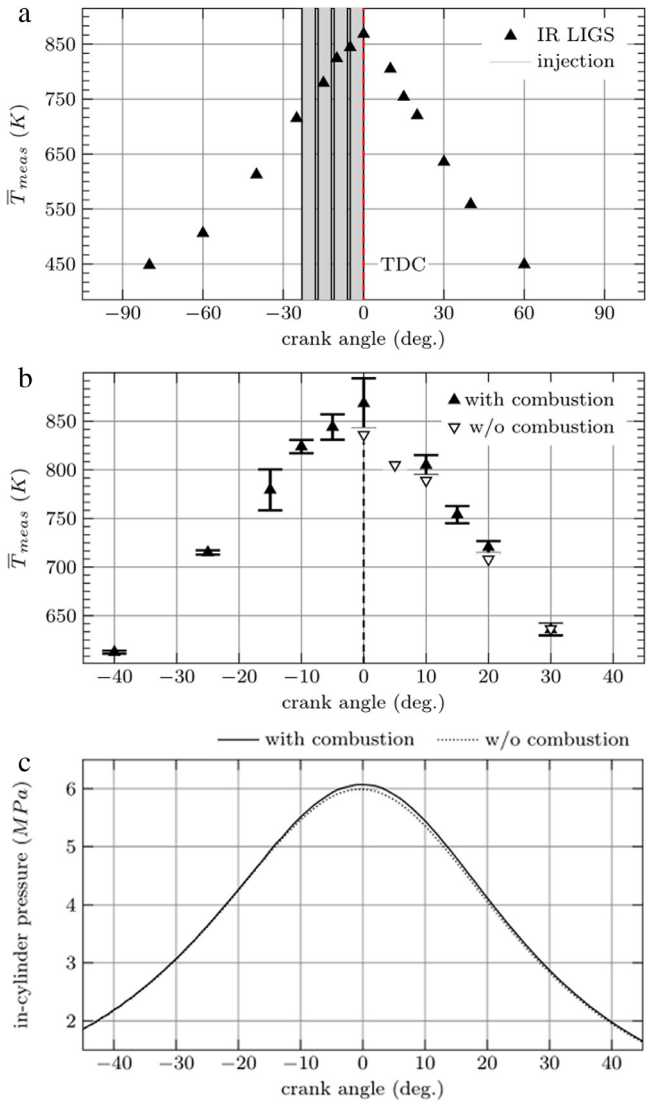

Fig. 6. (a) Crank angle-resolved measurements of temperature using IR-LIGS (LIEGS) showing the timing of the sequence of four injections of n-dodecane, between −30 and 0 CAD before TDC, to provide combustion by compression ignition. (see text for details). (b) Temperature values derived from LIEGS measurements during combusting (solid triangles) and non-combusting cycles (open triangles). Note the elevation of temperatures after TDC when combustion occurs relative to non-combusting cycles and the thermalization of the bulk temperature due to mixing as the expansion stroke progresses. (c) In-cylinder pressure during cycle recorded by pressure transducer. The very small difference in pressure during combustion cycles compared to non-combusting cycles is a result of the relatively small amount of fuel combusting in the large volume of the RCM.

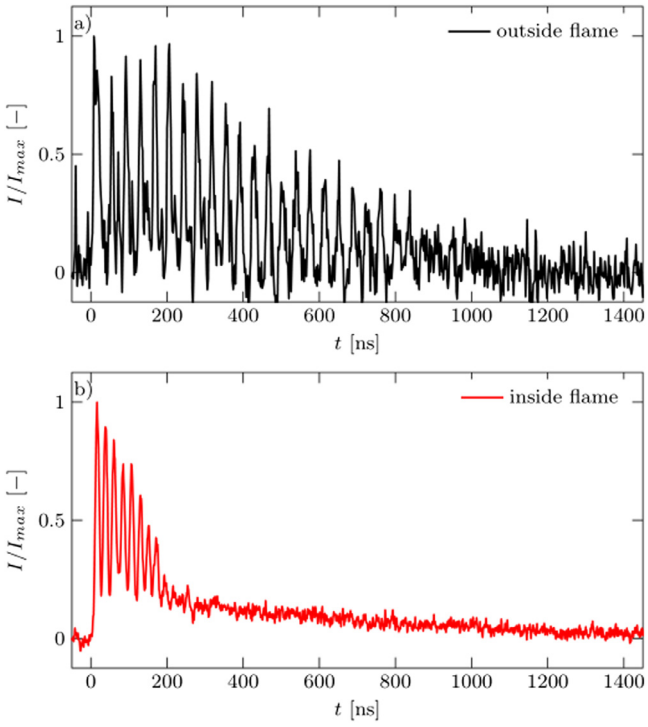

Fig. 7. (a) A typical LIEGS single-shot signal from the measurement volume during a combusting cycle. The observed oscillation frequency corresponds to a mean temperature of ~ 800 K. (b) A single-shot LIEGS signal showing rapid signal decay and higher oscillation frequency corresponding to a temperature of 2300 ± 100 K indicating a measurement in a flame or post-flame region.

estimated experimental error of ± 100 K compared to that in the non-combusting situations where the uncertainty is ± 15 K.

4. Conclusion

This work has demonstrated the first application of LIGS-based thermometry to measurements in compression-ignition or Diesel engine conditions. Measurements employing resonant LIGS by UV-excitation of thermal gratings with 1-methylnaphthalene as the absorber provided time-resolved temperature values during the compression and expansion stroke of a RCM in the absence of combustion. Non-resonant LIGS using IR-excitation provided a similar set of time-resolved measurements in excellent agreement with the values of those from the resonant absorption method. These non-resonant, LIEGS, signals also allowed the small temperature rise of the bulk gas resulting from combustion to be distinguished. In addition, direct measurements of flame or post-flame gases were observed in cycles where the random effects of turbulent gas flow carried the flame into the measurement region. Previous work has shown that use of a higher repetition-rate laser operating at 10 kHz would allow the present demonstration experiments to be extended to crank-angle-resolved measurements i.e. providing time-resolved data on the temperature evolution within the chamber [21]. In addition, other previous work demonstrated the capability of LIGS to make simultaneous measurements at multiple points i.e. giving spatial information on the temperature distribution [29]. The application of these techniques opens the possibility of time- and space-resolved study of combustion and flame development in compression-ignition engines.

The overall results have provided a high quality data set characterising the temporal evolution of temperature in the RCM that should prove useful for studies of spray, evaporation and mixing dynamics under Diesel-like engine conditions. The LIGS technique has thus been shown to provide robust data for the study of compression-ignition engines and information of importance for model validation and future engine design and development.

Acknowledgements

This work was supported in part by the Engineering and Physical Sciences Research Council (EPSRC), UK, [Grant nos. EP/M009424/1 and EP/K020528/1].

References

[1] A.C. Eckbreth, Laser diagnostics for combustion temperature and species, Gordon and Breach, 1996.
[2] E.B. Cummings, Laser-induced thermal acoustics: simple accurate gas measurements, Optics Lett. 19 (1994) 1361–1363.
[3] P.H. Paul, R.L. Farrow, P.M. Danehy, Gas-phase thermal-grating contributions to four-wave mixing, J. Optical Soc. Am. B 12 (1995) 384–392.
[4] W. Hubschmid, B. Hemmerling, A. Stampanoni-Panariello, Rayleigh and Brillouin modes in electrostrictive gratings, J. Opt. Soc. Am. B 12 (1995) 1850–1854.
[5] T.J. Butenhoff, E.A. Rohlfing, Laser-induced gratings in free jets. II. Photodissociation dynamics via photofragment transient gratings, J. Chem. Phys. 98 (1993) 5469–5476.
[6] S. Williams, L.A. Rahn, P.H. Paul, J.W. Forsman, R.N. Zare, Laser-induced thermal grating effects in flames, Optics Lett. 19 (1994) 1681–1683.
[7] H. Latzel, A. Dreizler, T. Dreier, J. Heinze, M. Dillmann, W. Stricker, G.M. Lloyd, P. Ewart, Thermal grating and broadband degenerate four-wave mixing spectroscopy of OH in high-pressure flames, Appl. Phys. B 67 (1998) 667–673.
[8] M.S. Brown, W.L. Roberts, Single-point thermometry in high-pressure, sooting, premixed combustion environments, J. Propuls. Power J. Propuls. Power 15 (1999) 119–127.
[9] B.A.O. Williams, M. Edwards, C.R. Stone, J. Williams, P. Ewart, High precision in-cylinder gas thermometry using laser induced gratings: quantitative measurement of evaporative cooling with gasoline/alcohol blends in a GDI optical engine, Combust. Flame 161 (2014) 270–279.
[10] B. Scott, C. Willman, B. Williams, P. Ewart, R. Stone, D. Richardson, In-cylinder temperature measurements using laser induced grating spectroscopy and two-colour PLIF, SAE Int. J. Eng. (2017), doi:10.4271/2017-24-0045.
[11] F. Förster, S. Baab, G. Lamanna, B. Weigand, Temperature and velocity determination of shock-heated flows with non-resonant heterodyne laser-induced thermal acoustics, Appl. Phys. B 121 (2015) 235–248.
[12] F. Förster, S. Baab, C. Steinhausen, G. Lamanna, P. Ewart, B. Weigand, Mixing characterization of highly underexpanded injection jets with real gas expansion, Exper. Fluids 59 (2018) 44.
[13] M. Meijer, B. Somers, J. Johnson, J. Naber, S-Y. Lee, L.M.C. Malbec, G. Bruneaux, L.M. Pickett, M. Bardi, R. Payri, T. Bazyn, Engine combustion network (ECN): characterization and comparison of boundary conditions for different combustion vessels, At. Sprays 22 (2012) 777–806, doi:10.1615/AtomizSpr.2012006083.
[14] O. Nilaphai, C. Hespel, B. Moreau, F. Contino, N. Bourgeois, S. Chanchaona, F. Foucher, C. Mounaïm-Rousselle, New high pressure and high temperature chamber for diesel spray characterization, 27th Annual Conference on Liquid Atomization and Spray Systems ILASS – Europe, Brighton, UK (2016).
[15] P. Desgroux, L. Gasnot, L.R. Sochet, Instantaneous temperature measurement in a rapid-compression machine using laser Rayleigh scattering, Appl. Phys. B 61 (1995) 69–72.
[16] G. Mittal, C-J. Sung, Aerodynamics inside a rapid compression machine, Combust. Flame 145 (2006) 160–180, doi:10.1016/j.combustflame.2005.10.019.
[17] B. Peterson, E. Baum, B. Böhm, V. Sick, A. Dreizler, Spray-induced temperature stratification dynamics in a gasoline direct-injection engine, Proc. Comb. Inst. 35 (2015) 2923–2931, doi:10.1016/j.proci.2014.06.103.
[18] W. Koban, J.D. Koch, R.K. Hanson, C. Schulz, Absorption and fluorescence of toluene vapor at elevated temperatures, Phys. Chem. Chem. Phys. 6 (2004) 2940–2945.
[19] B. Peterson, E. Baum, B. Böhm, V. Sick, A. Dreizler, Evaluation of toluene LIF thermometry detection strategies applied in an internal combustion engine, Appl. Phys. B 117 (2014) 151–175.
[20] C. Strozzi, J. Sotton, A. Mura, M. Bellenoue, Characterization of a two-dimensional temperature field within a rapid compression machine using a toluene planar laser-induced fluorescence imaging technique, Measur. Sci. Technol. 20 (2009) 125403.
[21] F.J. Förster, C. Crua, M. Davy, P. Ewart, Time-resolved gas thermometry by Laser Induced Grating Spectroscopy with a high-repetition rate laser system, Exper. Fluids 58 (2017) 87, doi:10.1007/s00348-017-2370-6.
[22] S. Baab, F. Förster, G. Lamanna, B. Weigand, Speed of sound measurements and mixing characterization of underexpanded fuel jets with supercritical reservoir condition using laser-induced thermal acoustics, Exper. Fluids 57 (2016) 172.
[23] C. Crua, Ph.D. Thesis, Combustion processes in a diesel engine, University of Brighton, UK, (2002) http://eprints.brighton.ac.uk/1161/.
[24] J. Kiefer, P. Ewart, Laser diagnostics and minor species detection in combustion using resonant four-wave mixing, Progr. Energy Combust. Sci. 37 (5) (2011) 525–564.

[25] E.W. Lemmon, M.L. Huber, M.O. McLinden, NIST standard reference database 23 (2013): reference fluid thermodynamic and transport properties-REFPROP, Version 9.1, National Institute of Standards and Technology, Standard Reference Data Program, Gaithersburg,
[26] J. Trost, L. Zigan, A. Leipertz, D. Sahoo, P.C. Miles, Characterization of four potential laser-induced fluorescence tracers for diesel engine applications, Appl. Optics 52 (33) (2013) 8001–8007.
[27] P. Ewart, C. Willman, B.A.O. Williams, J. Williams, C.R. Stone, High precision in-cylinder thermometry using laser induced grating spectroscopy, Institution of Mechanical Engineers Conference on Internal Combustion Engines (2015), p. 111. ISBN: 978-0-9572374-6-9.
[28] E.W. Lemmon, R.T. Jacobsen, S.G. Penoncello, D.G. Friend, Thermodynamic properties of air and mixtures of nitrogen, argon, and oxygen from 60 to 2000K at pressures to 2000MPa, J. Phys. Chem. Ref. Data 29 (3) (2000) 331–385.
[29] C. Willman, P. Ewart, Multipoint temperature measurements in gas flows using 1-D laser-induced grating scattering, Exper. Fluids 57 (2016) 191, doi:10.1007/s00348-016-2282-x.